JPET Fast Forward. Published on May 18, 2005 as DOI: 10.1124/jpet.105.085142
This article has not been copyedited and formatted. The final version may differ from this version.

Title Page

Pharmacological implications of two distinct mechanisms of interaction of memantine with NMDA-gated channels

Huei-Sheng Vincent Chen and Stuart A. Lipton

Center for Neuroscience and Aging, The Burnham Institute, La Jolla, California 92037 (H-S.V.C, S.A.L)

Departments of Cardiology (H-S.V.C) and Neurosciences (S.A.L.), University of California-San Diego, La Jolla, California 92037

Running Title Page

a) Running Title: Two mechanisms of memantine blockade at NMDA-gated channels

b) Corresponding author: Huei-sheng Vincent Chen

The Burnham Institute

10901 North Torrey Pines Road

La Jolla, California 92037

Tel. 858 646 3183

Fax 858 713 6273

Email: hsv_chen@burnham.org

c) Number of Text Pages: 21.5 pages (Introduction: 3, Materials and Methods: 5, Results: 8, and Discussion: 5.5).

Number of Tables: 1

Number of Figures: 6

Number of References: 39

Number of words in Abstract: 250

Number of words in Introduction: 749

Number of words in Discussion: 1498

d) A list of non-standard abbreviations: MEM, Memantine; NMDA, *N*-methyl-D-aspartate; MTS, methanethiosulfonate; MTSEA, 2-aminoethyl-methanethiosulphonate; NMG, *N*-methyl-D-glucamine; HME, Hexamethonium; MK-801, dizocilpine; PCP, phencyclidine.

Abstract

Unlike other NMDA receptor (NMDAR) antagonists, clinical trials have shown that memantine is clinically-tolerated and effective in the treatment of Alzheimer's disease. The mechanism for memantine tolerability, however, remains contentious but may be partly explained by its uncompetitive antagonism. The specific site of memantine block in the NMDAR-channel interacts with magnesium and is assumed to be at or near a narrow constriction representing the channel selectivity filter. A second, very low-affinity site of memantine action has also been reported. Here, using mutational analysis and substituted cysteine accessibility methods on recombinant NR1/NR2A NMDARs expressed in Xenopus oocytes, we precisely localize both the specific and second memantine-blocking sites. Intriguingly, memantine interacts with its specific-blocking site in the same fashion as intracellular rather than extracellular Mg^{2+}. Thus, the N-site asparagine (N) in the M2 region of the NR1 subunit represents the dominant site for uncompetitive antagonism by memantine. The N and N+1 site asparagines in NR2A produce strong electrostatic interactions with memantine. In contrast, the second (superficial) memantine-blocking site, located at the extracellular vestibule of the channel, appears to be non-specific and overlaps the site occupied by the non-specific pore blocker, hexamethonium. Residues in the post-M3 segment of the NR1 subunit are not directly involved in memantine binding. The distinct patterns of interaction and the relative degree of affinity of memantine for these two binding sites contribute to the drug's excellent pharmacological profile of clinical tolerability. In the future, these parameters should be considered in searching for improved neuroprotective agents in this class.

Introduction

N-methyl-D-aspartate-type glutamate receptors (NMDARs) are critical for normal functioning of the central nervous system (Nakanishi, 1992). Excessive activation of NMDARs by excitatory amino acids such as glutamate, however, contributes to neuronal damage in many neurological disorders (Choi, 1998; Lipton and Rosenberg, 1994). To avoid side effects, blockade of excessive NMDAR activity should be achieved without interfering with normal function. High-affinity NMDAR antagonists are toxic to neurons and produce neurobehavioral side effects (Rogawski and Wenk, 2003). In contrast, memantine is a low-affinity, uncompetitive open-channel blocker of the NMDAR and has excellent safety and efficacy profiles for treatment of Alzheimer's disease (Reisberg et al., 2003; Tariot et al., 2004). The molecular mechanism underlying the clinical tolerability of memantine remains contentious (Rogawski and Wenk, 2003; Lipton and Chen, 2004). Identification of the precise location(s) of memantine interaction on NMDARs would provide insight into the drug's clinical tolerability and aid in the search for better memantine-like agents.

We previously reported that memantine, at low micromolar concentrations, blocked NMDA-evoked responses via a bimolecular reaction and interacted with extracellular Mg^{2+} in NMDA-gated channels (Chen et al., 1992; Chen and Lipton, 1997). Because of its interaction with external Mg^{2+} and mutational analysis by others (Kashiwagi et al., 2002), the specific site of memantine action is assumed to be near the external Mg^{2+} blocking site at the selectivity filter region of the NMDAR-associated channel (Sakurada et al., 1993; Danysz and Parsons, 2003), which is formed by asparagine (N) residues at the "N-site" of NR1 and "N+1 site" of NR2 subunits

(Dingledine et al., 1999). Compared to physiological block by external Mg^{2+}, a common explanation for the safety and effectiveness of memantine is that memantine is a "better magnesium," manifesting a somewhat slower unblocking rate, moderate voltage dependence and slightly higher affinity (Danysz and Parsons, 2003). However, Mg^{2+} interacts differentially with the N-site residues of NR1 and NR2 subunits when applied from the intracellular versus extracellular surface (Wollmuth et al., 1998a, b). The N-site asparagine of the NR1 subunit represent the dominant blocking site for intracellular Mg^{2+}, whereas the N and N+1 site asparagines of the NR2A subunit form the critical blocking site for extracellular Mg^{2+}. Heretofore, the molecular interaction of memantine with these critical residues at the selectivity filter region has not been clearly demonstrated.

Additionally, using mutation/substitution analysis, Kashiwagi and colleagues (2002) showed that several residues in NR1 and NR2B affect antagonism by 1 μM memantine (on NR1: W608/W611 in the M2, residues near A645 in M3, and A653/V656/L657 in the post-M3 segments; on NR2B: W607L in the M2 segment). These residues, however, are located far apart, precluding the possibility that they all contribute to the binding site of 1 μM memantine. Here we demonstrate the mechanism by which these residues located in the channel selectivity filter and along the permeation pathway affect memantine action.

Several studies have also reported a second binding site for memantine in NMDA-gated channels (Antonov and Johnson, 1996; Blanpied et al., 1997; Bresink et al., 1996; Sobolevsky et al., 1998). This second site was reported to have a much lower affinity, minimal voltage-dependence, and a non-competitive mechanism of block. There

were, however, several differences among these studies, including the estimated IC_{50}, the precise degree of voltage dependence, and the location of this blocking site in the NMDA-gated channel. Additionally, memantine, unlike Mg^{2+} and MK-801, displays minimal NR2 subtype-specific difference for its blocking action among the various combinations of heteromeric NMDAR channels (Bresink et al., 1996). The influence of the eight splice variants of the NR1 subunit (Sugihara et al., 1992) on memantine blockade of NMDAR-associated channels remains unknown.

The aim of the present study was to precisely determine the molecular interaction of memantine on NR1/NR2A receptors at the specific binding site in the selectivity filter and to locate the second, very low-affinity site. Mutational analysis suggests that various open-channel blockers interact differently with the NMDAR channel permeation pathway (Kashiwagi et al., 2002). At the channel selectivity filter, however, a common assumption has been that all of these blockers act like extracellular Mg^{2+}. In contrast, our new results indicate that the predominant site for specific memantine action is at the blocking site for intracellular Mg^{2+} and not extracellular Mg^{2+}. The second, very low-affinity site is located at a shallow position in the extracellular vestibule that overlaps the site of action of non-specific blockers. The N- and N+1-site asparagines of the NR2A subunit stabilize memantine binding electrostatically. The pharmacological implications of our findings are discussed with regard to development of improved NMDAR antagonists.

Methods

Site-Directed Mutagenesis. Cloned cDNAs for the rat NMDAR subunits NR1a (pJS1, Sullivan et al., 1994) and NR2A (Monyer et al., 1992) were used as the template for all

mutations. We numbered the amino-acid residues beginning with the initiator methionine in the NR1 and NR2 clones (Moriyoshi et al., 1991). Thus, NR1(N616) and NR2A(N614) are the N site equivalents in the M2 region. The N to R mutant NR1(N616R) was obtained from Dr. R. Dingledine's laboratory (Emory University, Atlanta, Georgia). The remaining mutant NMDAR subunits were all generated in our laboratory using the PCR-based QuikChange™ Site-Directed Mutagenesis Kit (Stratagene). Multiple amino acid mutants on the same subunit were generated sequentially. All point mutations were verified by DNA sequencing of the mutated region (400 to 900 bps around the mutation site), and the whole clone was verified by restriction mapping. cRNA was transcribed *in vitro* using T3 or T7 mMESSAGE mMACHINE™ transcription kits (Ambion). The diagram in Figure 1A illustrates the relative positions of selected residues for mutations in the NR1 and NR2A subunits. Representative recordings of blockade by magnesium or various concentrations of amantadine and memantine of NMDA-evoked currents from wild-type or mutant NR1/NR2A channels are shown in Figure 1B.

Electrophysiological Recordings of Recombinant Channels from Oocytes. Preparation of Xenopus oocytes and injection of cRNA were performed as previously described (Choi et al., 2000). Whole-cell recordings were performed as previously described (Choi et al., 2000) at a holding potential of –60 mV unless otherwise indicated. The recording solution was comprised of Barium Ringer's solution (in mM): 1 $BaCl_2$, 95 NaCl, 2 KCl, 5 HEPES, pH adjusted to 7.5 with NaOH). 10 µM glycine and 200 µM NMDA were used to elicit NMDA-activated currents. Data were analyzed with MacLab v3.6 and Axograph v3.5.5 software (Axon Instruments). Solutions were applied to

oocytes with an array of pipettes similar to the "sewer pipe system" as described in Choi et al. (2000). All chemicals were purchased from Sigma unless otherwise indicated.

Protocols for Studying the Voltage Dependence of Memantine Block. As we previously described, intracellular monovalent permeant ions affect the apparent on-rate of memantine blockade, but this effect is minimal at holding potentials more negative than -60 mV (Chen and Lipton, 1997). Additionally, the effect of extracellular permeant ions on the on- and off-rates of memantine-like compounds is predominantly voltage independent (Antonov et al., 1998). At holding potentials more negative than –60 mV, the voltage-dependent ionic interactions would be minimized so that the true voltage-dependence of memantine blockade can be adequately assessed. Therefore, steady-state blockade by memantine at -60, -80, -100 and –120 mV was monitored to analyze the degree of voltage dependence of the various mutations.

Unlike other investigators, we avoided the voltage-ramp method to study the voltage-dependent effect of various mutations because, at voltages more positive than –60 mV, memantine binding shifts toward the shallow site and also manifests more complicated ionic interactions with intracellular permeant ions (Antonov et al., 1998). Therefore, δ (the electrical distance in Woodhull's model), calculated by the voltage-ramp method, represents the result of mixed-binding at the deep and shallow sites, as well as ionic interactions. Because of the difference in apparent IC_{50}s between uncompetitive and non-competitive blocking sites of memantine, 1μM memantine was used to assess voltage dependence in order to minimize any binding at the superficial, non-competitive site. If we found that the affinity of memantine decreased with a given point mutation, we used an increased memantine concentration of 10 μM for the determination of voltage

dependence. At these two concentrations and at holding potentials ≤-60 mV, memantine is a very specific open-channel blocker with 1:1 binding stoichiometry (Chen and Lipton, 1997). This type of action, displaying minimal voltage-dependence due to ionic interactions of permeant ions, approximates Woodhull's model (Woodhull, 1973). Each data point in the voltage-dependence analysis represents the mean ± SEM of the responses obtained from 3-7 oocytes.

Chemical Modification by MTSEA. The substituted cysteine accessibility method (SCAM) (Karlin and Akabas, 1998; Beck et al., 1999) was used to determine the location of residues that could affect memantine binding. For this purpose, we added the small sulfhydryl-modifying agent, 2-aminoethyl-methanethiosulphonate (MTSEA, Toronto Research Chemicals, Inc.), which reacts with free cysteine thiols to determine their accessibility after reaction with memantine. It should be noted, however, that a single endogenous cysteine residue, NR2A(C399), can be modified by MTSEA and would result in a decrease in NMDA-gated current that could obfuscate our results (Choi et al., 2000). To avoid this pitfall, in order to test the accessibility of cysteine-substituted mutants around the channel mouth, an NR2A(C399A) mutation was used in conjunction with other mutants to form heteromeric channels. For example, the NR2A(N614C) mutation was constructed with NR2A(C399A) as the template to generate the final mutant, NR2A(C399A/N614C).

The effect of MTSEA in the presence or absence of 200 μM memantine was assessed 15 s after the onset of memantine washout. This time point was chosen to allow ~90% recovery from memantine block while minimizing any significant recovery from MTSEA modulation. While assessing the protection from SCAM by memantine

(Protection- SCAM, Figs. 3 and 4), MTSEA was applied 10 s after memantine administration, and was subsequently washed out 15 s before memantine. In order to analyze the "on-rate" of MTSEA modification with a pulsatile protocol in the presence of an open-channel blocker like memantine, the washout rate of the open-channel blocker would have to be sufficiently fast to allow repeat application of MTSEA. Thus, we did not use a pulsatile protocol to monitor the on-rate of modification of exposed cysteines by MTSEA because the washout of millimolar concentrations of memantine is too slow, on the order of 6-8 min, in the oocyte recording system (Sobolevsky et al., 2002). However, this problem of slow washout will affect kinetic analyses but not steady-state analyses. In fact, a slow washout rate actually ensures the accuracy of Protection-SCAM analysis at steady state because memantine remains at the blocking site for a longer period. Therefore, in order to allow sufficient recovery from block by millimolar concentrations of memantine, the effect of MTSEA was measured 40 s after initiating washout of 2 mM memantine. For millimolar concentrations of hexamethonium, a multi-charged molecule, complete recovery from blockade occurs ~30 s after washout. Protection from MTSEA modulation by hexamethonium was therefore assessed at 15 and 30 s after washout.

Analysis of Dose-response and Voltage-dependence. Dose-response curves for inhibition by memantine, amantadine, or Mg^{2+} were determined by measuring steady-state currents after serial application of various concentrations of these compounds. The dose-response analysis was performed as described previously in detail (Chen and Lipton, 1997). Each point on the dose-response curve represents the mean ± S.E.M. of the response obtained from 3 to 12 oocytes. The data were weighted with the reciprocal

JPET Fast Forward. Published on May 18, 2005 as DOI: 10.1124/jpet.105.085142
This article has not been copyedited and formatted. The final version may differ from this version.

of the variance and fitted by SigmaPlot software using the Marquardt-Levenberg algorithm with an empirical Hill equation:

$$Y\ (\%) = 100 - \{Y_{max}/(1+(IC_{50}/[DRUG])^{n})\} \qquad (1)$$

where n is the empirical Hill coefficient, IC_{50} is the apparent 50% inhibition constant, and [DRUG] represents the concentration of various channel blocker drugs.

The voltage-dependence of inhibition by memantine was determined at various holding potentials by measuring the residual current after reaching a steady state of blockade with 1 μM or 10 μM memantine. The equilibrium dissociation constant (Ki) was calculated as previously described (Chen et al., 1992) using the following equation:

$$I_{control}/I_{MEM} = 1 + ([MEM]/Ki) / (1+EC_{50}/[NMDA]) \qquad (2)$$

where $I_{control}$ and I_{MEM} are defined as in Chen et al (1992), and EC_{50} is the apparent equilibrium dissociation constant for NMDA, which is assumed to be 50 μM. The Ki calculated from the degree of blockade was then fitted with the Woodhull equation (Woodhull, 1973) to estimate the fraction of the transmembrane field sensed by memantine (MEM):

$$Ki = Ki_{(0)} * \exp(V_H \delta z F/RT), \qquad (3)$$

where $Ki_{(0)}$ is the equilibrium dissociation constant for MEM at a holding potential of 0 mV; δ, the fraction of the transmembrane potential field sensed by extracellular application of MEM; V_H, the holding potential; z, the charge of MEM at neutral pH which is assumed to be +1 (Schneider et al., 1984); and F, R, and T have their usual meanings. Although the Woodhull equation is a simplified way to look at the voltage dependence of a channel blocker, it does allow us to compare the influence of the various N site mutants on the voltage dependence of memantine blockade.

JPET Fast Forward. Published on May 18, 2005 as DOI: 10.1124/jpet.105.085142
This article has not been copyedited and formatted. The final version may differ from this version.

Results

Interaction of memantine with the intracellular magnesium blocking site at the narrow constriction of the selectivity filter region

The specific memantine blocking site has been assumed to be near the narrow constriction region of the NMDAR-associated ion channel due to its interaction with extracellular Mg^{2+} as well as evidence from mutational analyses (Chen et al., 1992; Chen and Lipton, 1997; Kashiwagi et al., 2002). However, low micromolar concentrations of memantine have also been shown to interact with additional amino-acid residues in the M2, M3 and post-M3 segments of the NR1 subunit (Kashiwagi et al., 2002). Amino-acid substitutions for residues that lie in the permeation pathway could influence memantine action by direct, indirect or allosteric mechanisms of interaction. To determine more precisely the location of memantine action, we first investigated the effect of N-site mutations. Figure 1 shows the diagram of mutations and representative tracings as described in the Methods section. Q (glutamine) or R (arginine) substitution of the N-site asparagine in either NR1 or NR2A subunits decreases the degree of block by both extracellular and intracellular Mg^{2+} on recombinant NMDAR channels (Wollmuth et al., 1998a, b).

Figure 2A shows the dose-response curve for memantine block of 200 μM NMDA-activated currents on various combinations of mutant or wild-type heteromeric NMDAR channels. Figure 2A also shows that N to Q or R substitution in NR1 subunits decreases the potency of memantine blockade to a greater extent than the equivalent substitution in NR2A subunits. Although other residues may also contribute to

memantine binding to the specific site, this result suggests that the N-site residue in the NR1 subunit is the dominant site for memantine antagonism, resembling prior findings for block by intracellular Mg^{2+} (Wollmuth et al., 1998b). Additionally, the positively charged R substitution in either NR1 or NR2A reduced antagonism by memantine more than the equivalent Q substitution of the N-site asparagine.

In addition to the change in affinity of memantine antagonism caused by the various N-site mutations, Figure 2B demonstrates the change in voltage dependency that these mutations engendered. The assessments of memantine blockade were made at a number of steady-state holding potentials (see the Methods for details). The electrical distance from the extracellular surface of the membrane (δ) for each mutant was then calculated as described in the Methods. The N to Q substitution in the NR2A subunit moved the calculated δ by ~25% towards the extracellular side of the membrane's electrical field [from 0.84 for NR1/2A to 0.57 for NR1/NR2A(N614Q); or from 0.97 for NR1(N616Q)/NR2A to 0.73 for NR1(N616Q)/NR2A(N614Q)]. The N to Q mutation in the NR1 subunit, however, shifted the calculated δ ~14% towards the intracellular side of the membrane [from 0.84 for NR1/NR2A to 0.97 for NR1(N616Q)/NR2A; or from 0.57 for NR1/NR2A(N614Q) to 0.73 for NR1(N616Q)/NR2A(N614Q)]. These two opposite effects on electrical distance brought about by N to Q substitutions on NR1 versus NR2A subunits were additive if both subunits were mutated (i.e., if the N-site of NR1 and NR2A is each mutated to Q). Therefore, in comparison to NR1/NR2A wild-type receptors (with $\delta = 0.84$), the NR1(N616Q)/NR2A(N614Q) mutant (with $\delta = 0.73$) shifted δ towards the extracellular side of the membrane by 11% (= 25% - 14%). The effect on voltage dependence of the N to R mutation in the NR1 subunit was not tested because of the

requirement for much higher concentrations of memantine to achieve substantial blockade. At such high concentrations, memantine is not specific for the NMDAR open-channel blocking site (Chen et al., 1992 and see later section for Fig. 2D).

The asparagine residue at the N+1 position of the NR2 subunit (N615) forms part of the channel selectivity filter (Kuner et al., 1996; Wollmuth et al., 1996). However, N615Q mutation of the NR2A subunit decreased the IC_{50} of memantine blockade by only 6 fold (IC_{50} = 6.3 ± 1.8 □M), while dramatically decreasing the voltage dependence of block (δ = 0.40, Fig. 2B). The NR1/NR2A(N615R) combination resulted in no expression of functional heteromeric NMDA channels and therefore could not be tested further. Combining the affinity and voltage-dependence effects of mutations at the N- and N+1-sites on the NR2A subunit, we found that these two residues contribute only slightly to the specific binding site for memantine (as evidenced by their small effect on apparent affinity) but exert a predominant influence on the electrostatic interaction of memantine binding (as seen by their effect on voltage dependence). Interestingly, these two NR2A residues have been shown to affect block by intracellular Mg^{2+} in a similar manner (Wollmuth et al., 1998b). In contrast, the dramatic effect of mutation of the N-site asparagine of the NR1 subunit on memantine affinity leads us to conclude that this residue (also representing the intracellular Mg^{2+} blocking site) is the predominant memantine blocking site.

We also tested the effect on memantine blockade of mutating residues around the N-site asparagine in the M2 region of the NR1 subunit. In agreement with a recent study characterizing many such residues (Kashiwagi et al., 2002), we found that S604A, S617N, and G618D mutations in the M2 domain of the NR1 subunit, which affect

JPET Fast Forward. Published on May 18, 2005 as DOI: 10.1124/jpet.105.085142
This article has not been copyedited and formatted. The final version may differ from this version.

blockade by external Mg^{2+} or PCP (Yamakura et al., 1993), exert minimal effects on the specific memantine channel-blocking site. W611L mutation of the NR1 subunit decreased memantine affinity slightly as well as voltage dependence (δ= 0.63). Mutation of the A645 residue to serine in the M3 domain of the NR1 subunit, which affects MK-801 affinity, decreased the IC_{50} of memantine by 4 fold without changing its voltage dependence (δ= 0.8). The tryptophan residue (W606L) at the –8 position from the N-site of the NR2A subunit, unlike its effect on NR1/NR2B receptors (Kashiwagi et al., 2002), decreased memantine blockade by only two fold (IC_{50} = 1.5 ± 0.9 μM) and slightly increased the voltage-dependence (δ= 0.88).

Use of Protection-SCAM to locate the memantine binding sites

In order to locate precisely the memantine binding sites on the NMDARs, we present in Figure 3 a modified method for protecting exposed cysteine residues with memantine from reaction with methanethiosulfonate (MTS) agents (Protection-SCAM, see also Sobolevsky et al., 2002). The NR1(N616C) mutation decreased the IC_{50} of memantine to 40 μM (Fig. 2C) due to the critical role of the N-site on the NR1 subunit for specific memantine binding. In contrast, the NR2A(N614C) N-site mutation manifested a smaller effect on the potency of memantine (IC_{50} = 1.4 ± 0.6 μM) and decreased voltage dependence of block (δ= 0.45). This result is consistent with the finding above that the N-site asparagine of NR2A affects memantine action primarily via electrostatic interaction. Since the N-site asparagines of the NR1 and NR2 subunits are located close together (Amar et al., 2001), we used the NR2A(N614C) mutant, which manifests less effect on affinity than the NR1 mutant, to determine if memantine can prevent accessibility of MTS agents to the region controlling the channel selectivity filter.

C399A was included in this mutant [NR2A(C399A/N614C)] to avoid reaction of MTS with endogenous C399 (see Methods). The NR2A(C399A) mutation did not affect the affinity or voltage dependence of memantine action.

A relatively high concentration of memantine (200 μM) was used in this experiment to ensure blockade of 100% of the specific memantine binding sites (on the other hand, ≤30% of the non-specific sites were blocked by this concentration, Fig. 2A). We found that memantine prevented most of the effect of 20 μM MTSEA on the NR2A N-site mutant. To show this, we measured residual NMDA-evoked current after the addition of MTSEA in the presence and absence of memantine (Fig. 3A). To compare the effect of memantine on the various single cysteine-substituted mutants in the channel mouth, we measured the parameter of relative degree of modulation (block or potentiation) by MTSEA in the presence or absence of memantine (designated the "relative degree of MTSEA modulation" or ***RDM***; Fig. 3). MTSEA reacted with NR2A(N614C) and blocked the current by 79.5 ± 1.6%. Using the RDM, we found that memantine prevented 86.8 ± 3.1% of this MTSEA modulation. This result confirms that the selectivity filter region is the major site for specific memantine action (Chen and Lipton, 1997; Kashiwagi et al., 2002; Sobolevsky et al., 2002). Note that measurement of the slowing of the on-rate of MTSEA action by memantine was not used in this study because of the relatively slow washout of memantine in the oocyte expression system (for details, see Materials and Methods).

Location of a second site of memantine action

As mentioned earlier, there appears to be a second, very low affinity site for memantine action, and amino-acid residues in the M3 and post-M3 segments of the NR1 subunit can

affect this blocking action of memantine. In agreement with the results of Beck et al. (1999), we found that MTSEA decreased the current of NR1(L651C)/NR2A(C399A), NR1(F654C)/NR2A(C399A), and NR1(R659C)/NR2A(C399A) channels, yet potentiated the current of NR1(A653C)/NR2A(C399A) channels. In order to locate the second, very low-affinity site of memantine action, the relative degree of modulation (RDM) was calculated for cysteine-substituted mutants in the channel mouth using higher concentrations of memantine. N to R substitution in NR2A changed the δ of memantine block to ~0.5, a value similar to that of non-specific polar organic ions such as Tris (δ = 0.51) and NMG (δ = 0.51) (Villarroel et al., 1995). The value of δ for NR1(L651C), NR1(A653C) and NR1(F654C) mutations after exposure to MTS reagents was ≥0.3, 0.0, and 0.0, respectively (Sobolevsky et. al., 2002). We thus hypothesized that these residues must be located at or near the outer edge of the second, non-specific site of memantine binding at the channel vestibule.

From the dose-response curve for memantine inhibition of NR1(N616R)/NR2A (Fig. 2A), we knew that 200 μM memantine blocked ~30% of the non-specific sites while 2 mM blocked ~90%. These two concentrations were therefore chosen to more precisely locate the second site of memantine action using Protection-SCAM. We found that 200 μM memantine prevented 50-60% of the modulation by MTSEA at L651C, A653C and F654C (Fig. 4B, left-hand panel). However, increasing the concentration of memantine to 2 mM protected L651C from MTSEA modulation even better. Nonetheless, we observed that there was less protection by 2 mM memantine as the location of the cysteine moved in the extracellular direction (residues A653C and F654C), suggesting

that the second site of memantine binding was located at or very near L651 and internal to F654C (Fig. 4B, *right-hand panel).*

For the post M3 segment, we know from previous work that V656A and L657A mutations of the NR1 subunit affect the potency of memantine (Kashiwagi et al., 2002). The L657C mutation was minimally modified by MTSEA in our study. Therefore, the more externally located R659C mutation of NR1 was used to assess memantine protection from SCAM. However, we found that 2 mM memantine offered no protection of the R659C residue from reaction with MTSEA (Fig. 4B, *right-hand panel*). As a technical note for these experiments, the residues for cysteine substitution were chosen because of their spatial proximity to the second memantine binding site, which influenced MTSEA modulation but did not significantly alter memantine affinity per se (data not shown).

Significance and non-specific nature of the second site of memantine action

Hexamethonium (HME) is an acetylcholine receptor blocker that can non-specifically block the NMDAR channel at millimolar concentrations at –100 mV (Villarroel et al., 1995). We found that 2 mM and 20 mM HME, at a holding potential of –100 mV, blocked NMDA-gated current by ~50% and 90%, respectively. We then used the Protection-SCAM technique described above to localize the site of non-specific HME binding in the NMDAR channel. NR1(L651C) modulation was slightly affected by 2 mM HME, while 20 mM drastically reduced L651C modulation. In contrast, 2 mM HME did not affect modulation of A653C or F654C, and 20 mM had only a modest effect (30-40% protection), suggesting that A653 and F654 are located at the outer edge of the HME binding site (Fig. 5). Additionally, the residue R659C in the post-M3 segment of

the NR1 subunit was not protected from MTSEA modulation by 20 mM HME. Thus, the non-specific site of HME binding is virtually the same as the non-specific site of memantine action.

In order to further understand the significance of this second site of memantine block, we investigated the potency of amantadine, a memantine analog, in blocking NMDA-activated currents. We chose amantadine for this experiment because of its similarity in structure and size with memantine, which suggests that these two drugs interact with the NMDAR in a similar manner. For NR1/NR2A heteromeric channels, the dose-response data at -60 mV yielded an IC_{50} of 0.9 μM for memantine blockade and an IC_{50} of 34 μM for amantadine. R substitution at the N-site of the NR1 subunit shifted the dose-response curves for memantine and amantadine to the right, resulting in an IC_{50} of ~300 μM and ~700 μM, respectively. Since at hundreds of micromolar, both memantine and amantadine exhibit effects on other receptors (Chen et al., 1992), these results suggest that this block is relatively non-specific and that dose-response curves for memantine and amantadine approach similar values after losing their interaction with the specific binding site in the channel. Furthermore, we suggest that the ratio of affinities between the specific and non-specific blocking sites for amantadine (20 fold) is too small compared to memantine (300 fold) to allow clinical application of amantadine as a specific and clinically-tolerated NMDA antagonist (Fig. 2D). We speculate that the method of comparing affinities between sites demonstrated in Figure 2D will prove useful in searching for additional clinically-tolerated, “low-affinity” open-channel blockers (see Discussion).

Lack of effect of variant NR1 isoforms on memantine potency

The experiments described above were all performed with the NR1-1a splice variant, which has two C-terminal inserts and no N-terminal insert. We therefore co-expressed NR1-1b (containing all N- and C-terminal inserts), NR1-4a (lacking all N- and C-terminal inserts), or NR1-4b (containing only the N-terminal insert) with NR2A to form heteromeric channels in the oocyte expression system. None of the NR1 splice variants differentially affected the affinity of memantine antagonism. Neither was the voltage dependence of memantine blockade differentially influenced (Table 1).

Discussion

In this study, we used point mutations and SCAM to show the N-site asparagine of the NR1 subunit at the selectivity filter of the NMDAR-associated channel is the specific and predominant blocking site for memantine. The N and N+1 sites of NR2A subunits provide the major electrostatic interaction with memantine upon binding to this deep, specific site. The differential contribution to memantine block by the N- and N+1 site asparagines in NR1 and NR2 subunits is reminiscent of their effects on intracellular Mg^{2+} blockade (Wollmuth et al., 1998b). Additionally, a second, more superficial site for memantine antagonism that manifests a much lower affinity is located on NR1 at the level of residue L651. This second site appears to be non-specific and overlaps the site occupied by non-specific pore blockers, such as hexamethonium. We show that a large difference in the affinity between these two sites is crucial for maintaining the selectivity of a “low-affinity” NMDAR open-channel blocker like memantine. Finally, we find amino-acid residues in the more external post-M3 segment are not directly involved in memantine binding.

Many possible factors have been suggested for memantine's clinical tolerability, including moderate-to-low affinity, fast unblocking kinetics, and moderate voltage dependence in the NMDAR-associated channel (Rogawski and Wenk, 2003). These macroscopic explanations suggest that memantine acts like a "better magnesium" based on comparison with the kinetic properties of block by "extracellular" Mg^{2+} at the channel selectivity filter (Danysz and Parsons, 2003). In the present study, however, we show that this comparsion may be misleading. Instead, memantine interacts with the intracellular Mg^{2+} blocking site, which is located slightly deeper than the extracellular Mg^{2+} blocking site (Kuner et al., 1996). This finding clearly indicates that memantine should not be simply considered a "better external Mg^{2+} blocker."

Our experiments on the voltage dependence of memantine blockade revealed further details of the molecular interaction of memantine with amino-acid residues in the selectivity filter region. N-to-Q substitution at the N-site of the NR2A subunit shifted the calculated δ ~25% towards the extracellular side of the membrane electric field. In contrast, the N-to-Q mutation at the N-site of the NR1 subunit [NR1(N616Q)] shifted the calculated δ approximately 14% towards the "intracellular" side. These two opposing effects on electrical distance were additive if both subunits were mutated. One possible explanation for this opposing effect on the calculated $\delta$is that the carbonyl oxygen in the N-site of the NR2A subunit points towards the extracellular side of the membrane, while the carbonyl oxygen in the N-site of the NR1 subunit points intracellularly.

Furthermore, the NR1(N616Q) mutation affected the voltage dependence of memantine blockade less than half that of the equivalent substitution on the NR2A subunit. A simple model (Fig. 6) suggests that the carbonyl oxygen of the N-site on the

NR1 subunit is located relatively horizontal to the long axis of the channel pore, while the carbonyl oxygen side chain of the NR2A N-site manifests a more vertical orientation. We also found that the N-to-Q mutation at the N+1 site of the NR2A subunit decreased the calculated δ more than the N-site substitution, suggesting a steric effect in addition to a simple electrostatic interaction and compatible with a critical role of the N+1 site in forming the selectivity filter. The differential orientation of carbonyl oxygens in NR1 and NR2A subunits at the channel selectivity filter may explain why other open-channel blockers differ in their pharmacological properties from memantine if they predominantly interact with the extracellular Mg^{2+} site. To support this concept, we modeled the M2-to-M3 segment of the NR1 subunit as an inverted K^+ channel based on the latter's crystal structure. The resulting model showed that the orientation of the carbonyl oxygen of the N-site of the NR1 subunit is very close to that proposed here. Due to a staggered configuration relative to the NR1 subunit (Wollmuth and Sobolevsky, 2004), the M2-to-M3 segments of the NR2A subunit cannot be simply modeled in this manner (see legend Fig. 6).

Furthermore, the reduced voltage dependence of memantine action after N-to-Q mutation at the N or N+1 sites of the NR2A subunit suggests that the externally pointing carbonyl oxygens provide significant electrostatic stabilization of memantine when it is bound to the N-site of the NR1 subunit. Conceivably, this electrostatic stabilization would affect many drug properties such as slowing the unblocking rate, changing the voltage dependence, and enhancing trapping of memantine. This complex effect may explain why prior studies, focused on low-affinity, slow kinetics of block, voltage-dependence, and partial trapping, have not identified a single factor for the tolerability of

memantine (Parsons et al., 1995). The true molecular binding site(s) of other open-channel blockers and their interaction with NMDARs should be further investigated in order to find a safer and more effective antagonist.

Other studies have shown that amino-acid residues in addition to the N-site asparagine in the M2 and M3 segments of NR1 and NR2 subunits affect Mg^{2+} and memantine blockade of NMDARs (Dingledine et al., 1999; Kashiwagi et al., 2002). In the present study, we performed assays of both affinity and voltage dependence in order to assess the effects of these other amino-acid substitutions on memantine blockade. We found that residues located near the selectivity filter region in either the M2 or M3 segment of NR1(W611 and A645) or NR2A(W606) slightly affected the affinity or voltage dependence of memantine blockade. This result is consistent with the notion that these residues exert an allosteric effect on memantine action.

We also precisely located a second, superficial binding site for memantine near the level of residue L651 in the M3 segment of the NR1 subunit. Amino-acid residues located externally to NR1(F654) were not protected by memantine even at very high (millimolar) concentrations in the Protection-SCAM assay and are therefore not directly involved in memantine binding. In contrast to our results, A653T in the M3 segment and V656A, L657A in the post-M3 segment of NR1, were reported to decrease antagonism by 1 μM memantine (Kashiwagi et al., 2002). However, the A653C and L657C residues manifest differential modification rates by MTSEA in the open versus closed conformation (Sobolevsky et al., 2002). Thus, these externally located residues are more likely to be involved in a conformational change during channel gating. Their mutations,

therefore, may alter the structure or the open-closed equilibrium of the permeation pathway, resulting in a change in affinity of various open-channel blockers.

Alternatively, the effect of the NR1(A653T) mutation might suggest that binding of memantine to this superficial site is required prior to a rapid transition into the deeper selectivity-filter site (Antonov et al., 1998). At low micromolar concentrations and hyperpolarized potentials, this latter scenario would have minimal significance after considering the very low affinity of memantine (>300 μM at –60 mV) at this superficial site, which would result in such an ephemeral dwell time that it would preclude any physical meaning. However, this transition may become more significant for very low affinity open-channel blockers, like amantadine, and at more depolarized potentials, such as pathological depolarization by toxic levels of glutamate.

Additionally, we established a simple method using NR1(N616R) versus the wild-type NR1 subunit to quickly evaluate the relative affinity between the two sites of memantine action (as in Fig. 2D). For so called "low-affinity" NMDA open-channel blockers, the apparent affinity, apparent unblocking rate, and degree of trapping of each open-channel blocker will represent "mixed" properties of both sites if the relative affinities are not too far apart. Therefore, despite prior reports, none of these properties at one site alone can explain the variable clinical tolerability of low-affinity NMDAR antagonists. In the case of memantine, however, the affinities of the two sites are sufficiently distinct that the pharmacological properties of the specific site may account for its lack of side effects (Lipton and Chen, 2004).

Another important therapeutic implication of our findings concerns uncompetitive antagonism. Uncompetitive, unlike competitive or non-competitive, antagonists can

block excessive activation of NMDARs while sparing normal neurotransmission (Lipton and Chen, 2004). Memantine blocks NMDARs via an uncompetitive mechanism at low micromolar concentrations, yet possesses a non-competitive component (via partial trapping in the channel) at higher concentrations (Blanpied et al., 1997; Chen and Lipton, 1997). Lipophilic leak of memantine from its blocking site cannot explain this non-competitive component (Mealing et al., 2001; Bolshakov et al., 2003). Instead, here we identify a second site of memantine binding of very low affinity at the channel vestibule. Occupancy by memantine of this shallow site may allow dissociation of the drug in either the open or closed conformation, resulting in a form of non-competitive antagonism. This superficial site of memantine action is non-specific and may also explain the non-competitive component of many other very low-affinity, open-channel blockers. Importantly, we describe a method to rapidly evaluate the relative affinity of drugs between the superficial and deep sites of the NMDAR. This relative affinity may be used to predict the "non-competitive" versus "uncompetitive" component of action of an NMDAR channel blocker, and therefore will be an important tool in the search for future therapeutic agents in this class.

Acknowledgments:

The authors thank Akira Wada for excellent technical assistance and Hiroto Takahashi for computer modeling of the NMDA-gated channel.

References

Amar M, Perin-Dureau F, Neyton J (2001) High-affinity Zn block in recombinant N-methyl-D-aspartate receptors with cysteine substitutions at the Q/R/N site. *Biophys J* **81**:107-116.

Antonov SM, Johnson JW (1996) Voltage-dependent interaction of open-channel blocking molecules with gating of NMDA receptors in rat cortical neurons. *J Physiol* **493**:425-445.

Antonov SM, Gmiro VE, Johnson JW (1998) Binding sites for permeant ions in the channel of NMDA receptors and their effects on channel block. *Nat Neurosci* **1**:451-461

Beck C, Wollmuth LP, Seeburg PH, Sakmann B, Kuner T (1999) NMDAR channel segments forming the extracellular vestibule inferred from the accessibility of substituted cysteines. *Neuron* **22**:559-570.

Blanpied TA, Boeckman FA, Aizenman E, Johnson JW (1997) Trapping channel block of NMDA-activated responses by amantadine and memantine. *J Neurophysiol* **77**:309-323.

Bolshakov KV, Gmiro VE, Tikhonov DB, and Magazanik LG (2003) Determinants of trapping block of *N*-methyl-D-aspartate receptor channels. *J Neurochem* **87**:56-65.

Bresink I, Benke TA, Collett VJ, Seal AJ, Parsons CG, Henley JM, Collingridge GL (1996) Effects of memantine on recombinant rat NMDA receptors expressed in HEK 293 cells. *Br J Pharmacol* **119**:195-204.

Chen HS, Pellegrini JW, Aggarwal SK, Lei SZ, Warach S, Jensen FE, Lipton SA (1992) Open-channel block of N-methyl-D-aspartate (NMDA) responses by memantine:

therapeutic advantage against NMDA receptor-mediated neurotoxicity. *J Neurosci* **12**:4427-4436.

Chen HS and Lipton SA (1997) Mechanism of memantine block of NMDA-activated channels in rat retinal ganglion cells: uncompetitive antagonism. *J Physiol* **499**:27-46.

Choi DW (1998) Antagonizing excitotoxicity: A therapeutic strategy for stroke? *Mt Sinai J Med* **65**:133-138.

Choi YB, Tenneti L, Le DA, Ortiz J, Bai G, Chen HS, Lipton SA (2000) Molecular basis of NMDA receptor-coupled ion channel modulation by S-nitrosylation. *Nat Neurosci* **3**:15-21.

Danysz W and Parsons CG (2003) The NMDA receptor antagonist memantine as a symptomatological and neuroprotective treatment for Alzheimer's disease: preclinical evidence. *Int J Geriatr Psychiatry* **18**(Suppl 1):S23-S32.

Dingledine R, Borges K, Bowie D, Traynelis SF (1999) The glutamate receptor ion channels. *Pharmacol Rev* **51**:7-61.

Karlin A and Akabas MH (1998) Substituted-cysteine accessibility method. *Methods Enzymol* **293**:123-145.

Kashiwagi K, Masuko T, Nguyen CD, Kuno T, Tanaka I, Igarashi K, Williams K (2002) Channel blockers acting at *N*-methyl-D-aspartate receptors: differential effects of mutations in the vestibule and ion channel pore. *Mol Pharmacol* **61**:533-545.

Kuner T, Wollmuth LP, Karlin A, Seeburg PH, and Sakmann B (1996) Structure of the NMDA receptor channel M2 segment inferred from the accessibility of substituted cysteines. *Neuron* **17**:343-352.

Lipton SA, Rosenberg PA (1994) Mechanisms of disease: Excitatory amino acids as a final common pathway for neurologic disorders. *N Engl J Med* **330**:613-622.

Lipton SA, Chen HS (2004) Paradigm shift in neuroprotective drug development: clinically tolerated NMDA receptor inhibition by memantine. *Cell Death Diff* **11**:18-20.

Mealing GA, Lanthorn TH, Small DL, Murray RJ, Mattes KC, Comas TM, Morley P (2001) Structural modifications to an N-methyl-D-aspartate receptor antagonist result in large differences in trapping block. *J Pharmacol Exp Ther* **297**:906-914.

Monyer H, Sprengel R, Schoepfer R, Herb A, Higuchi M, Lomeli H, Burnashev N, Sakmann B, Seeburg PH (1992) Heteromeric NMDA receptors: molecular and functional distinction of subtypes. *Science* **256**:1217-1221.

Moriyoshi K, Masu M, Ishii T, Shigemoto R, Mizuno N, Nakanishi S (1991) Molecular cloning and characterization of the rat NMDA receptor. *Nature* **354**:31-37.

Nakanishi S (1992) Molecular diversity of glutamate receptors and implications for brain function. *Science* **258**:597-603

Parsons CG, Quack G, Bresink I, Baran L, Przegalinski E, Kostowski W, Krzascik P, Hartmann S, Danysz W (1995) Comparison of the potency, kinetics and voltage-dependency of a series of uncompetitive NMDA receptor antagonists in vitro with anticonvulsive and motor impairment activity in vivo. *Neuropharmacology* **34**:1239-1258

Reisberg B, Doody R, Stoffler A, Schmitt F, Ferris S, and Mobius HJ-Memantine Study Group (2003) Memantine in moderate-to-severe Alzheimer's disease. *N Engl J Med* **348**:1333-1341.

Rogawski MA and Wenk GL (2003) The neuropharmacological basis for the use of memantine in the treatment of Alzheimer's disease. *CNS Drug Rev* **9**:275-308.

Sakurada K, Masu M, Nakanishi S (1993) Alteration of Ca2+ permeability and sensitivity to Mg2+ and channel blockers by a single amino acid substitution in the N-methyl-D-aspartate receptor. *J Biol Chem* **268**:410-415.

Schneider E, Fischer PA, Clemens R, Balzereit F, Fünfgeld EW, Haase HJ (1984) Wirkungen oraler Memantingaben auf die Parkinsonsymptomatik. *Dtsch Med Wochenschr* **109**:987.

Sobolevsky AI, Koshelev SG, Khodorov BI (1998) Interaction of memantine and amantadine with agonist-unbound NMDA-receptor channels in acutely isolated rat hippocampal neurons. *J Physiol* **512**:47-60.

Sobolevsky AI, Beck C, Wollmuth LP (2002) Molecular rearrangements of the extracellular vestibule in NMDAR channels during gating. *Neuron* **33**:75-85.

Sugihara H, Moriyoshi K, Ishii T, Masu M, Nakanishi S (1992) Structures and properties of seven isoforms of the NMDA receptor generated by alternative splicing. *Biochem Biophys Res Commun* **185**:826-832.

Sullivan JM, Traynelis SF, Chen HS, Escobar W, Heinemann SF, Lipton SA (1994) Identification of two cysteine residues that are required for redox modulation of the NMDA subtype of glutamate receptor. *Neuron* **13**:929-936.

Tariot PN, Farlow MR, Grossberg GT, Graham SM, McDonald S, Gergel I; Memantine Study Group (2004) Memantine treatment in patients with moderate to severe Alzheimer disease already receiving donepezil: a randomized controlled trial. *J Am Med Assoc* **291**:317-324.

Villarroel A, Burnashev N, Sakmann B (1995) Dimensions of the narrow portion of a recombinant NMDA receptor channel. Biophys *J* **68**:866-875.

Wollmuth LP, Kuner T, Seeburg PH, and Sakmann B (1996) Differential contribution of the NR1- and NR2A-subunits to the selectivity filter of recombinant NMDA receptor channels. *J Physiol* **491**:779-797.

Wollmuth LP, Kuner T, and Sakmann B (1998a) Adjacent asparagines in the NR2-subunit of the NMDA receptor channel control the voltage-dependent block by extracellular Mg^{2+}. *J Physiol* **506**:13-32.

Wollmuth LP, Kuner T, Sakmann B (1998b) Intracellular Mg^{2+} interacts with structural determinants of the narrow constriction contributed by the NR1-subunit in the NMDA receptor channel. *J Physiol* **506**:33-52.

Wollmuth, LP, Sobolevsky, AI (2004) Structure and gating of the glutamate receptor ion channel. *Trends Neurosci* **27**:321-328.

Woodhull AM (1973) Ionic blockage of sodium channels in nerve. *J Gen Physiol* **61**:687-708.

Yamakura T, Mori H, Masaki H, Shimoji K, Mishina M (1993) Different sensitivities of NMDA receptor channel subtypes to non-competitive antagonists. *NeuroReport* **4**:687-690.

Footnotes

This work was supported in part by an American Heart Association Scientist Development Grant to H-S V. Chen, NIH grants P01 HD29587, R01 EY09024, and R01 EY05477, and a Senior Scholar Award from the Ellison Medical Foundation to S. A. Lipton.

JPET Fast Forward. Published on May 18, 2005 as DOI: 10.1124/jpet.105.085142
This article has not been copyedited and formatted. The final version may differ from this version.

Legends for Figures

Figure 1. Diagram of NR1 and NR2A mutations and recordings from mutant channels.

(A) Schematic representation of the NR1 and NR2A subunits indicating the location of mutated amino-acid residues studied here. The N-site and N+1 site asparagine residues are numbered**.**

(B) Representative recordings showing inhibition of 200 μM NMDA-evoked currents from wild-type and mutated NR1/NR2A channels by 100 μM Mg^{2+} or various concentrations of memantine (MEM) and amantadine. Horizontal scale bar, 30 s for all traces. Vertical scale bar, 200 nA except for NR1/NR2A(N615Q), where the scale bar is 50 nA. *Lower left*: An example of the technique used to measure steady-state voltage dependence of memantine blockade is illustrated

Figure 2. Dose-response curve and voltage dependence of memantine block by various mutations of the channel filter region of NR1/NR2A receptors.

(A) Blockade of 200 μM NMDA-evoked currents in oocytes by various concentrations of memantine (MEM) at a holding potential of -60 mV. Various amino-acid mutations of the N-site in the M2 region of NR1 and/or NR2A subunits decrease MEM blockade of NMDA-evoked responses. Fractional response (%, as defined in the Methods section) was used to construct the dose-response curves.

(B) Voltage dependence of calculated Ki in the presence or absence of N-site or N+1 site substitutions. The δ (electrical distance from the extracellular side of the membrane) was 0.84 for NR1/NR2A, 0.97 for NR1(N616Q)/NR2A, 0.57 for

NR1/NR2A(N614Q), 0.73 for NR1(N616Q)/NR2A(N614Q), 0.50 for NR1/NR2A(N614R), and 0.40 for NR1/NR2A(N615Q).

(C) Effect of cysteine substitution at the N-site of NR1 and NR2 subunits. Substitution at the NR1 N-site decreased the IC_{50} of memantine blockade to a much greater extent than the equivalent mutation in the NR2A subunit. Each point represents the mean ±SEM of the responses obtained from 8-9 oocytes.

(D) Dose-response analysis of memantine and amantadine blockade of 200 μM NMDA-evoked responses by wild-type (WT) and NR1(N616R)/NR2A mutant channels. The amantadine dose-response curve was constructed as in A (mean ± SEM; n = 3-7 for each data point), and representative recording traces are shown in Fig. 1B.

Figure 3. Protection of an exposed cysteine residue in the N-site of the NR2A subunit by memantine (MEM).

(A) Two-electrode voltage clamp recordings from NR1/NR2A(C399A,N614C) channels are shown. Memantine potency was minimally affected when compared to wild-type NR1/NR2A channels. The protocol described below was used to study protection of exposed cysteines by memantine from MTS reagents. Peak amplitude of NMDA/glycine (200/10 μM)-gated current was measured prior to memantine application (Ipre). Residual current after blockade (Ipost) was measured 15 s after washout of 200 μM memantine. The ratio of Ipost to Ipre [$(Ipost/Ipre)_{MEM}$] represents the degree of residual current after memantine blockade, and [$(Ipost/Ipre)_{MTSEA+MEM}$] represents the residual current after memantine and MTSEA exposure. MTSEA (20 μM) was applied for 40 s, the minimal time

required to reach steady-state modulation of NR1/NR2A(C399A/N614C) channels under our conditions.

(B) *Left-hand panel*: Residual current after memantine alone, MTSEA alone, or both drugs. To calculate the true percentage of residual current remaining after exposure to MTSEA plus memantine, we had to correct for the blockade that remained 15 s after washout of memantine alone (seen in Column B, Fig. 3B). We accomplished this by taking the ratio of $(Ipost/Ipre)_{MTSEA+MEM}$ (Column C) to $(Ipost/Ipre)_{MEM}$ (Column B), resulting in the value shown in Column C/B, which represents the true percentage of residual current remaining after MTSEA treatment in the presence of memantine. In order to compare the degree of protection afforded by memantine from MTSEA modulation among the various mutated NMDAR-channels, we established a parameter termed the "relative degree of modulation" (designated the "RDM"). *Right-hand panel*: The RDM after MTSEA exposure in the presence and absence of memantine was calculated by comparing current modulation by MTSEA plus memantine [100% minus C/B% (residual current) = E in *left-hand panel*] to modulation by MTSEA alone (= D in *left-hand panel*). A smaller RDM indicates a higher degree of protection from MTSEA by memantine. In the case of NR1/2A(C399A,N614C) channels, MTSEA blocked the current by 79.5 ± 1.6% (= D). With co-application of 200 μM memantine, MTSEA blocked the current only 10.6 ± 2.6% (= E). The RDM (= E/D) was 13.2 ± 3.1%, indicating that 200 μM memantine allowed only 13% of the normal MTSEA modulation (n = 7).

Figure 4. Protection by memantine (MEM) of exposed cysteine residues at the extracellular vestibule of the NR1 subunit.

(A) Heteromeric channels consisting of NR1 mutants and NR2A(C399) subunits were tested using a protocol similar to that of Fig. 3A. Two representative tracings of MTSEA modulation of NMDA/glycine (200/10 μM)-gated currents are shown. MTSEA (20 μM) decreased the current amplitude of NR1(F654C)/NR2A (C399A) channels (*top tracing*), but potentiated the current of NR1(A653C)/ NR2A(C399A) channels (*bottom tracing*). A higher concentration of MTSEA (200 μM) was used for NR1(L651C)/NR2A(C399A) channels in order to produce a similar degree of modulation as for the other mutant channels tested here. The vertical scale bar represents 100 nA and the horizontal bar, 10 s.

(B) Histograms of RDM for various NR1 cysteine mutants. *Left-hand panel:* 200 μM memantine efficiently protected the cysteine residue from MTSEA modulation in the channel filter region [NR2A(N614C)], but provided much less protection of cysteine residues in the extracellular vestibule. *Right-hand panel:* Protection from MTSEA modulation by a high concentration of memantine (2 mM) was virtually complete at the second site of memantine action, representing very low-affinity blockade [NR1(L651)]. Decreasing protection from MTSEA by memantine (a so-called "edge effect," manifest as a rising RDM) was observed for cysteine mutations located more externally, e.g., NR1(R659C), and hence farther away from the very low-affinity site (see Model in Fig. 6). RDM (in %) for each cysteine mutant is presented as the mean ±SEM of the responses obtained from 5-8 oocytes.

Figure 5. Protection of exposed cysteine residues at the extracellular vestibule (M3 and Post-M3 segments) of the NR1 subunit by Hexamethonium (HME).

(A) Heteromeric channels consisting of NR1 mutants and NR2A(C399) subunits were tested using a protocol similar to that of Fig. 3A. Representative recordings illustrate protection by HME from MTSEA modulation of cysteine residues. The vertical scale bar represents 100 nA and the horizontal bar, 10 s. A high concentration of HME (20 mM) afforded more protection of the exposed cysteine in NR1(F654C)/NR2A(C399A) channels than a lower concentration (2 mM).

(B) Histograms of RDM for various NR1 cysteine mutants in the presence of HME (mean ± SEM, n = 3-7 for each group). *Left-hand panel:* 2 mM HME protected the cysteine residue from MTSEA modulation at the L651 position but provided no protection to the more external residues (A653 and F654) at the extracellular vestibule. The RDM was 60.9±6.9 % for NR1(L651C)+2A(C399A). *Right-hand panel:* Protection by 20 mM HME from MTSEA modulation was most pronounced at the NR1(L651C) residue. The most distant residue from L651 in this series, represented by R659C, which is located at the extracellular surface, was not protected at all, even by this very high concentration of HME. The RDM was 39.3±8.5 % for NR1(L651C)+2A(C399A).

Figure 6. Atomic model showing two memantine binding sites in the channel permeation pathway of the NMDAR.

The model incorporates data from point mutations and Protection-SCAM studies. Yellow arrows indicate the likely orientation of the carbonyl oxygen atoms of the N and N+1 site asparagines. Locations of memantine binding sites in the channel

permeation pathway are shown at the level of the channel selectivity filter and the L651 residue of the NR1 subunit (memantine molecules are outlined in gray). For clarity, only the M1, M2 (pore loop), and M3 segments are shown here. To model the NMDAR channel, we submitted a sequence of transmembrane fragments of the NR1 subunit to the Genesilico Fold Prediction Metaserver. This procedure allowed us to discern the best available solved crystal structure for this region. The ffas algorithm of this program, which assigns peptide folds based on the profile-profile method, scored Ksca and Kvap potassium channels the highest, consistent with the assumptions of sequence and structural homology between NMDAR and K^+ channels. After aligning the NMDAR subunit sequence with Ksca and Kvap, we used Swiss-Model software to model tertiary structure of the M2-to-M3 regions of the NR1 subunit as an inverted K^+ channel based on the known crystal structures of these two K^+ channels (PDB IDs 1jvm and 1orq, respectively). The Iterative Magic Fit function was then performed, and the resulting geometry was further compared and aligned. However, the NR2 subunit cannot be modeled in this fashion because it is not symmetrically aligned with the NR1 subunit at the M2 and M3 regions (Kuner et al., 1996; Wollmuth and Sobolevsky, 2004). Therefore, we manually generated a model for the NR2A subunit using the computer program 3DSMAX (Discreet) in conjunction with the NR1 model and empirical data suggesting differential orientation of carbonyl oxygens between the two subunits.

JPET Fast Forward. Published on May 18, 2005 as DOI: 10.1124/jpet.105.085142
This article has not been copyedited and formatted. The final version may differ from this version.

Table 1

Effect of NR1 isoforms on the IC_{50} and voltage dependence of memantine blockade

IC_{50} values were obtained from dose–response curves as described in the Methods; Ki(0) and δ were obtained during steady-state memantine blockade at various holding potentials using the Woodhull model as described in the Methods section.

Mutant Channels	**IC_{50}**	**Ki (0)**	□
NR1-1a/NR2A Wild Type	0.79±0.20	4.89± 2.21	0.84
NR1-1b/NR2A	0.94±0.29	6.99± 1.42	0.85
NR1-4a/NR2A	0.87±0.19	4.30± 2.84	0.84
NR1-4b/NR2A	1.10±0.14	5.37± 1.06	0.83

Figure 1

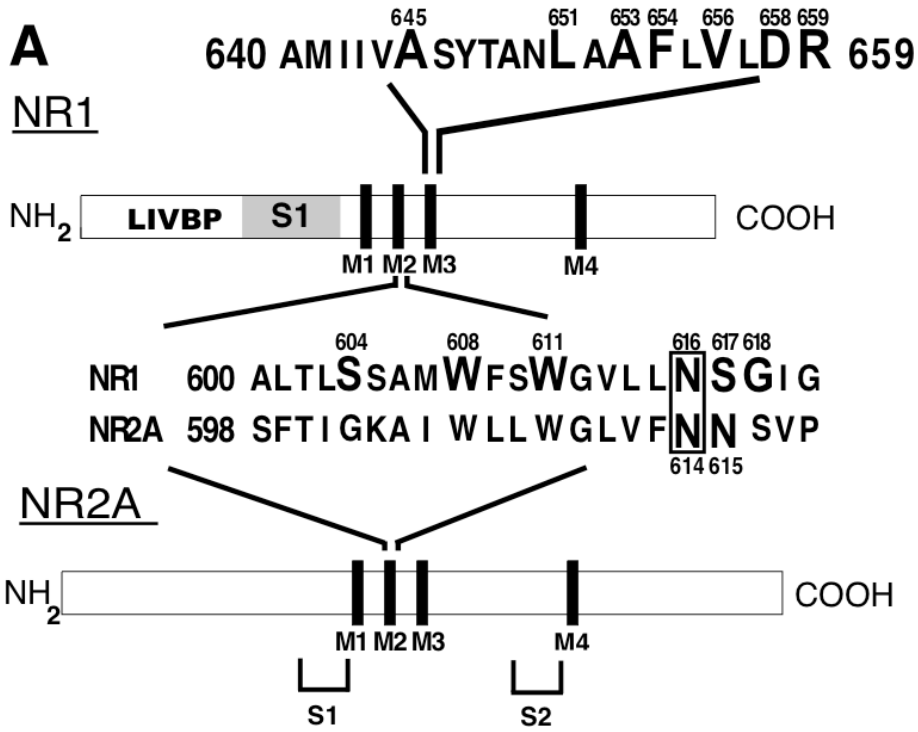

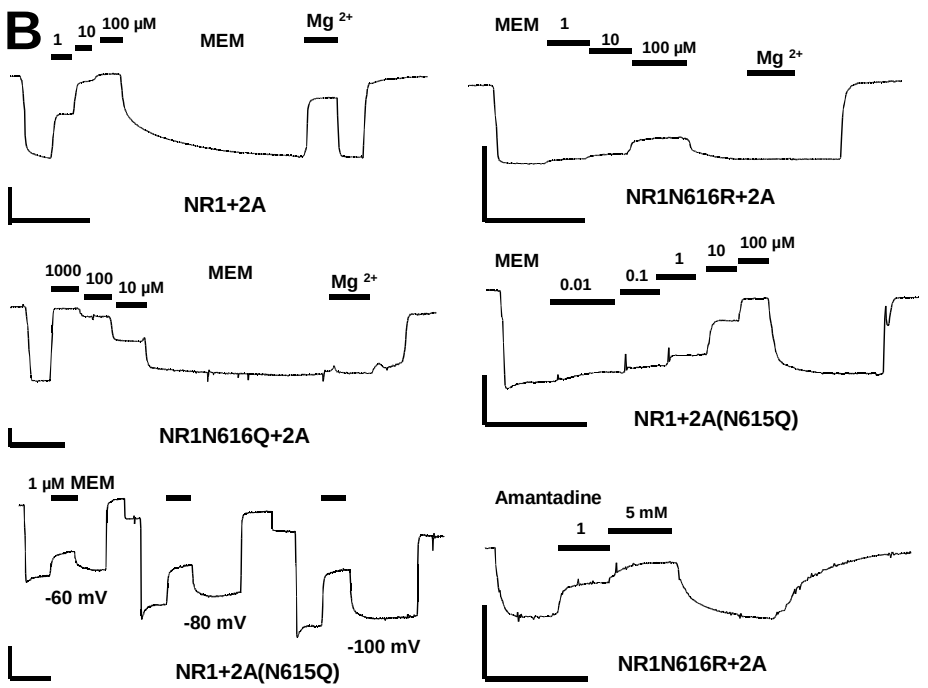

Figure 2

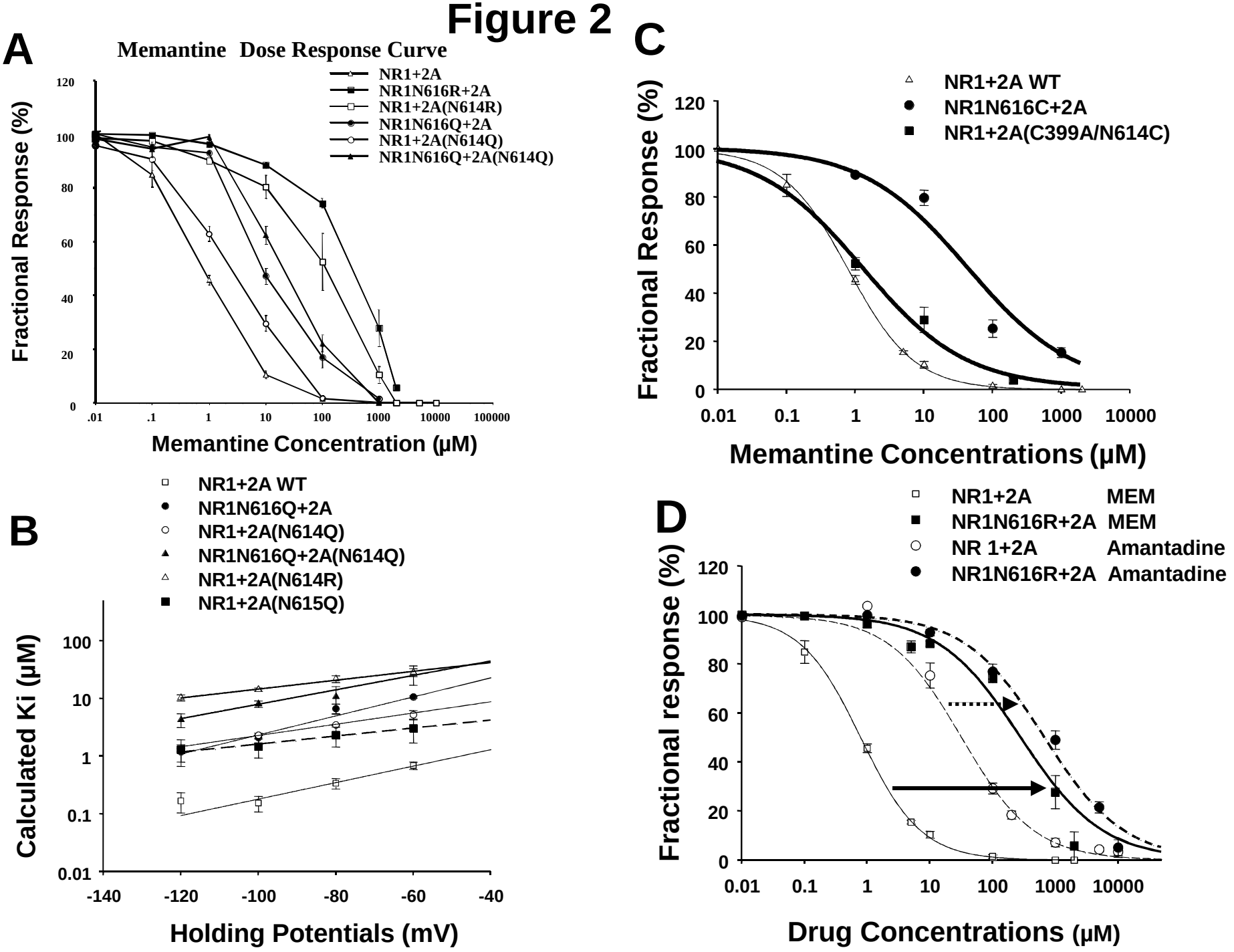

Figure 3

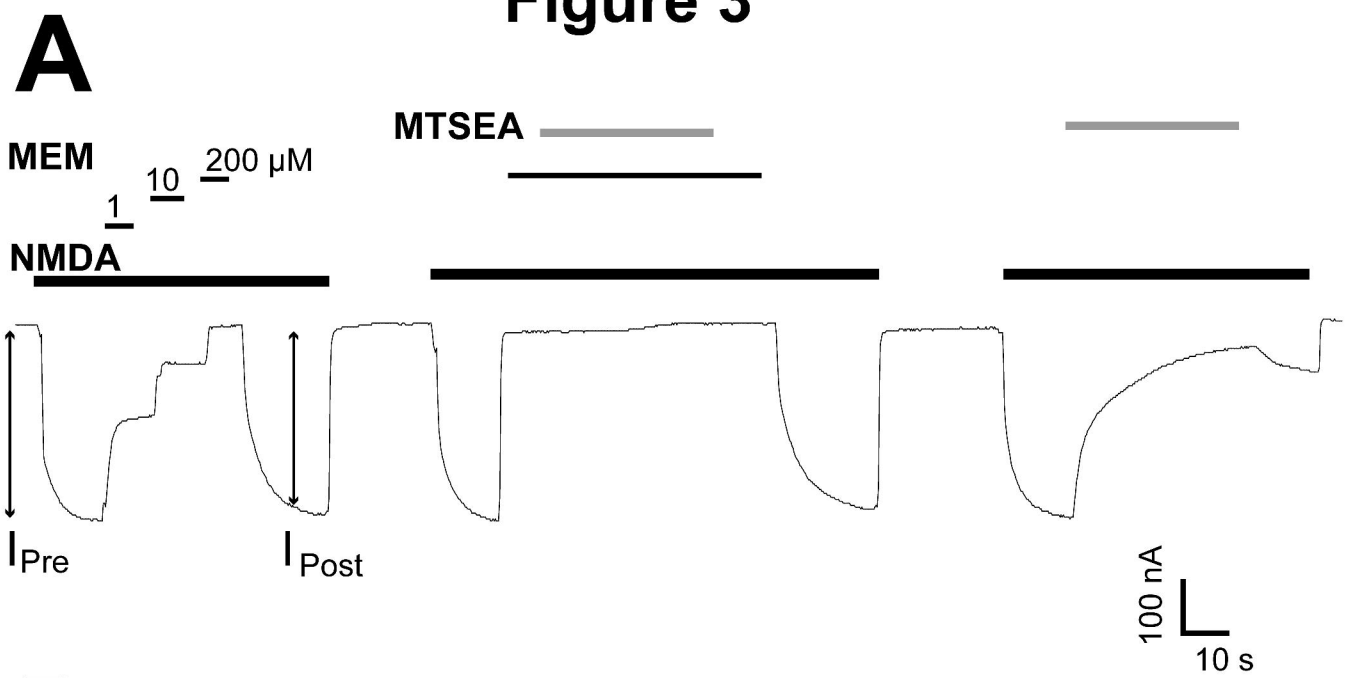
A
MTSEA
MEM
10
200 μM
1
NMDA
Pre
Post
100 nA
10 s

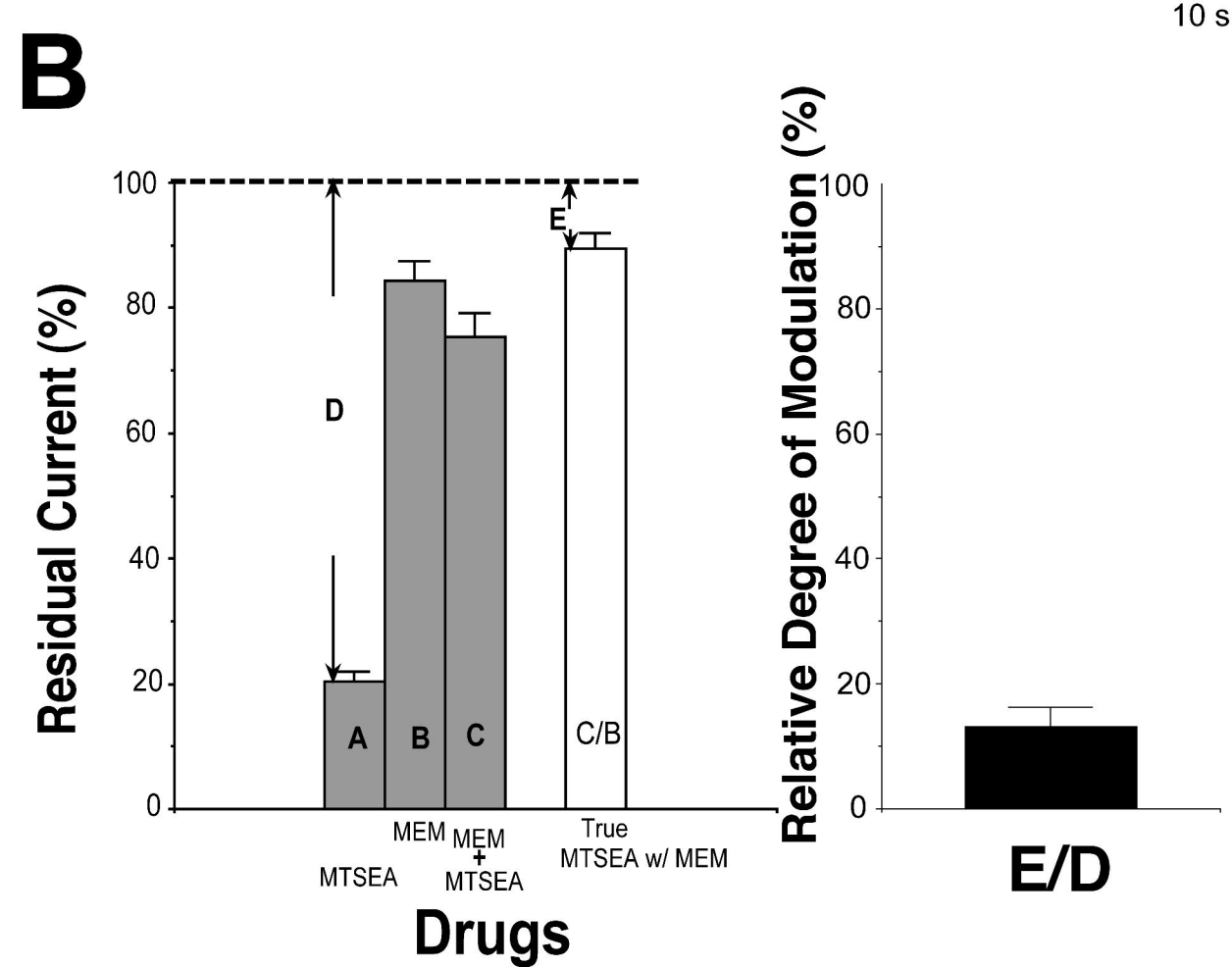
B
Residual Current (%)
100
80
60
40
20
0
D
E
A
B
C
C/B
MTSEA
MEM
MEM + MTSEA
True MTSEA w/ MEM
Drugs
Relative Degree of Modulation (%)
E/D

Figure 4

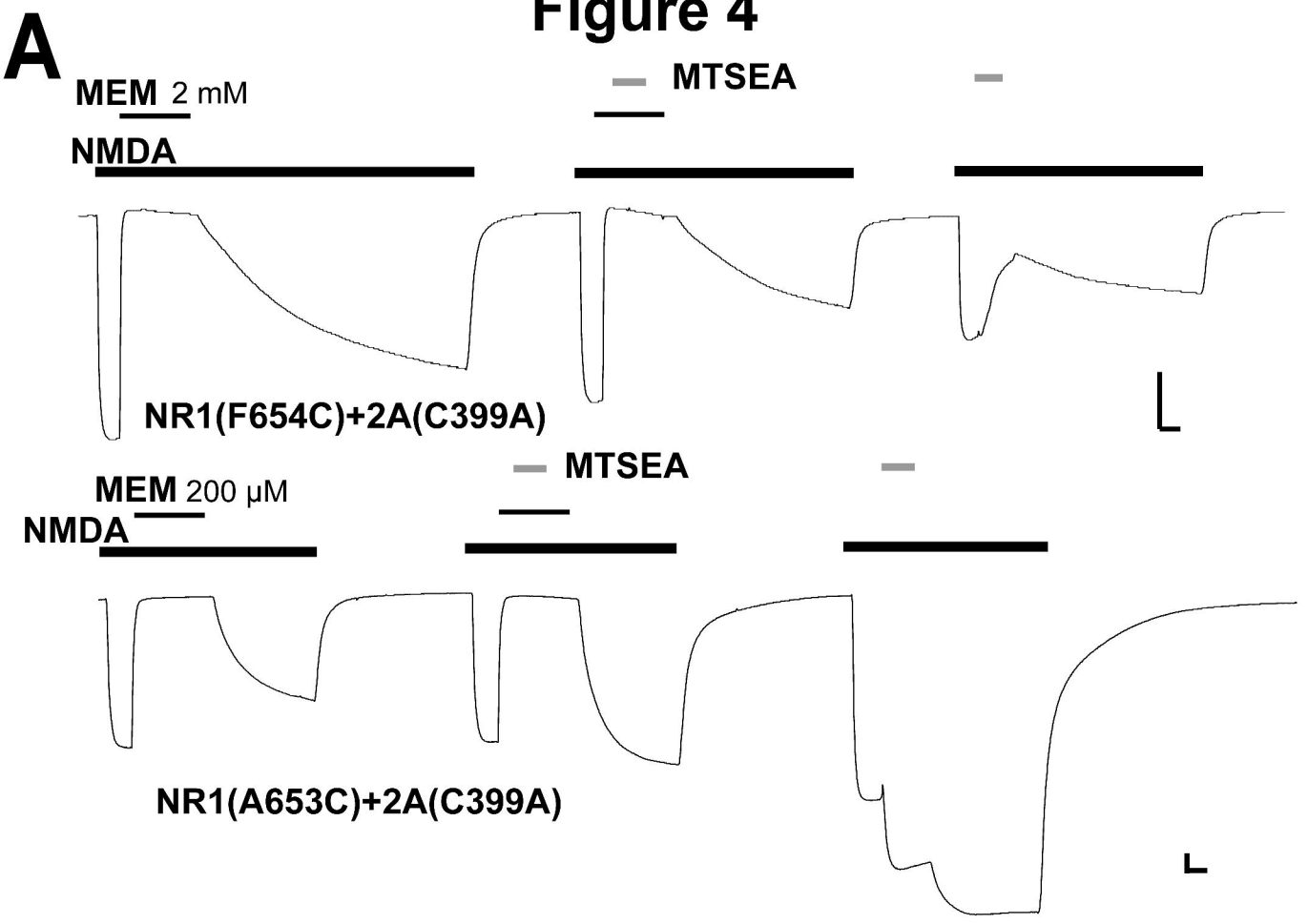
A
MEM 2 mM
MTSEA
NMDA
NR1(F654C)+2A(C399A)
MTSEA
MEM 200 µM
NMDA
NR1(A653C)+2A(C399A)

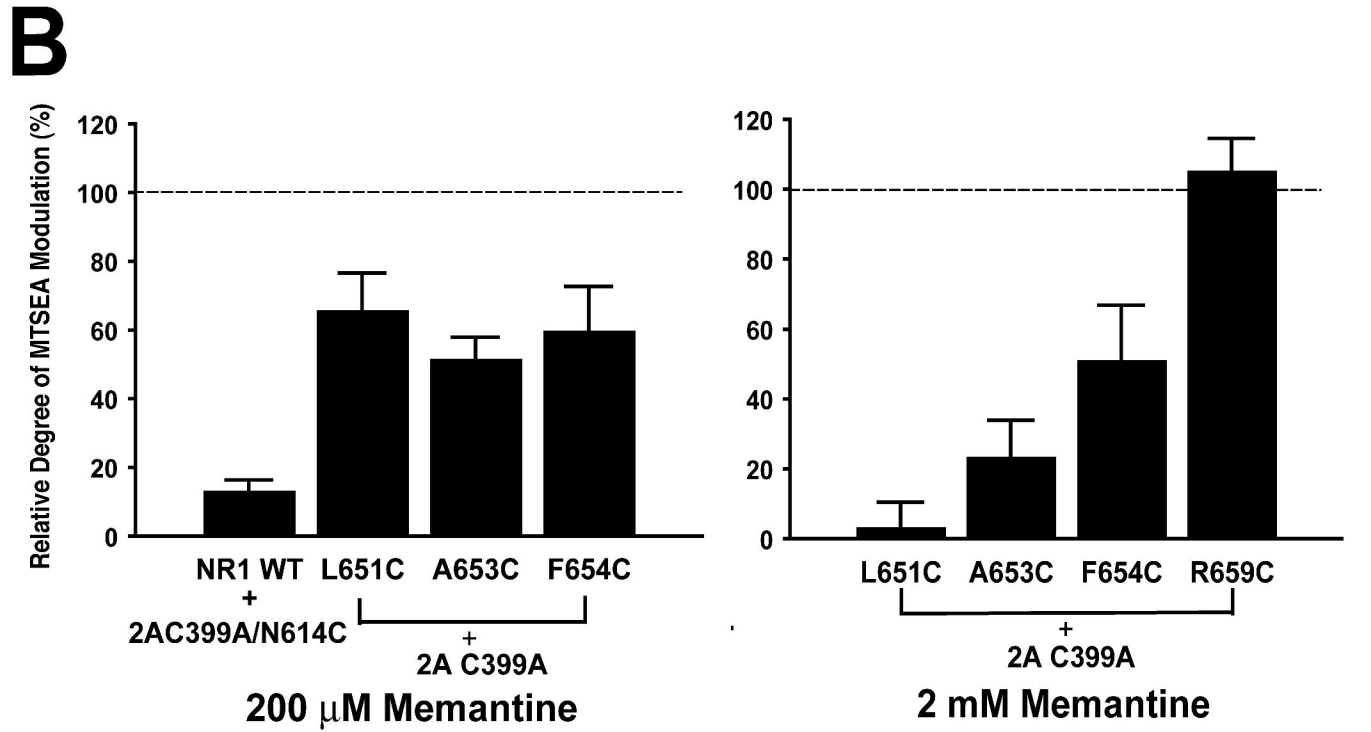
B
Relative Degree of MTSEA Modulation (%)
120
100
80
60
40
20
0
NR1 WT + 2AC399A/N614C
L651C + 2A C399A
A653C + 2A C399A
F654C + 2A C399A
200 µM Memantine
L651C + 2A C399A
A653C + 2A C399A
F654C + 2A C399A
R659C + 2A C399A
2 mM Memantine

Figure 5

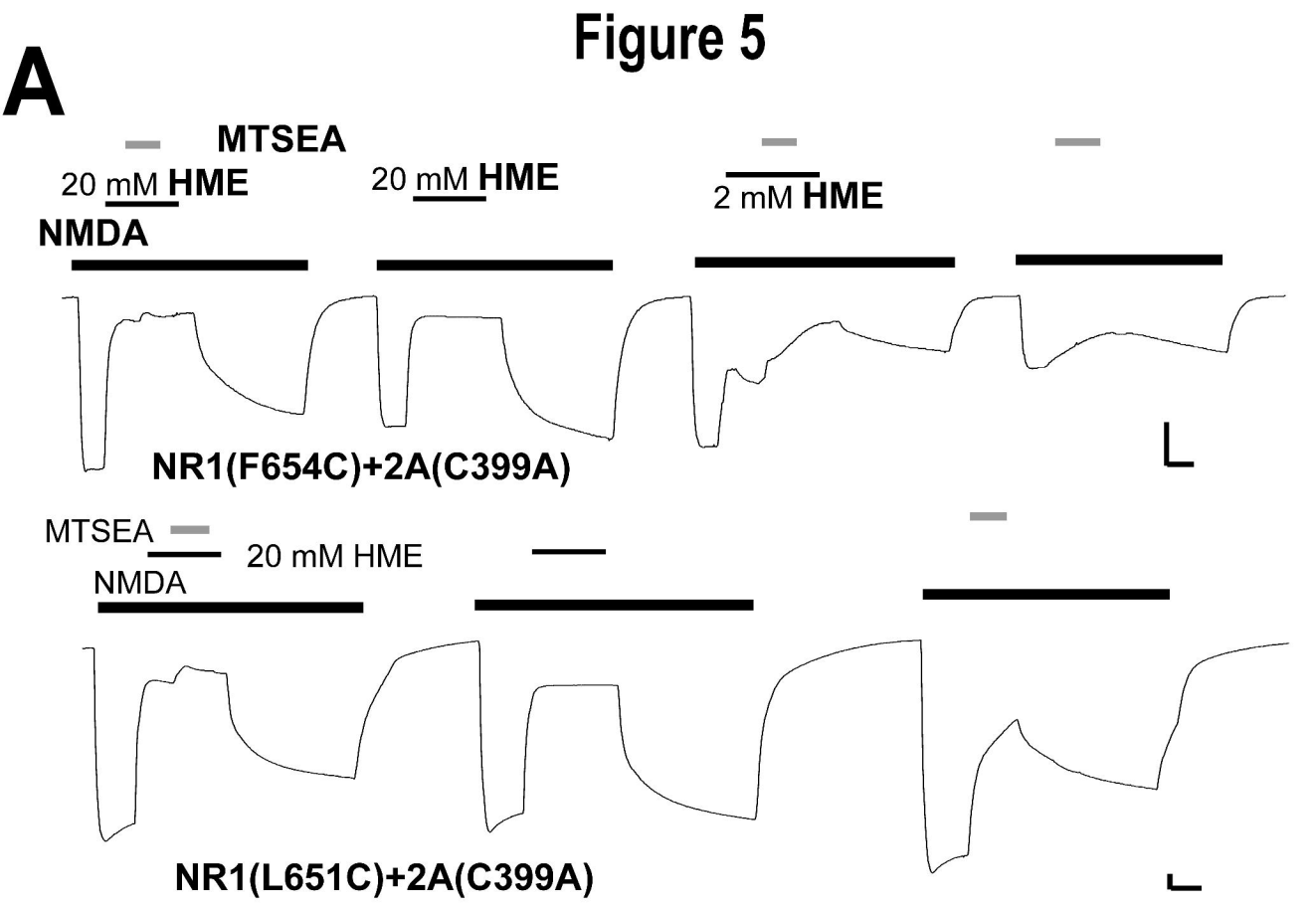
A
MTSEA
20 mM HME
20 mM HME
2 mM HME
NMDA
NR1(F654C)+2A(C399A)
MTSEA
20 mM HME
NMDA
NR1(L651C)+2A(C399A)

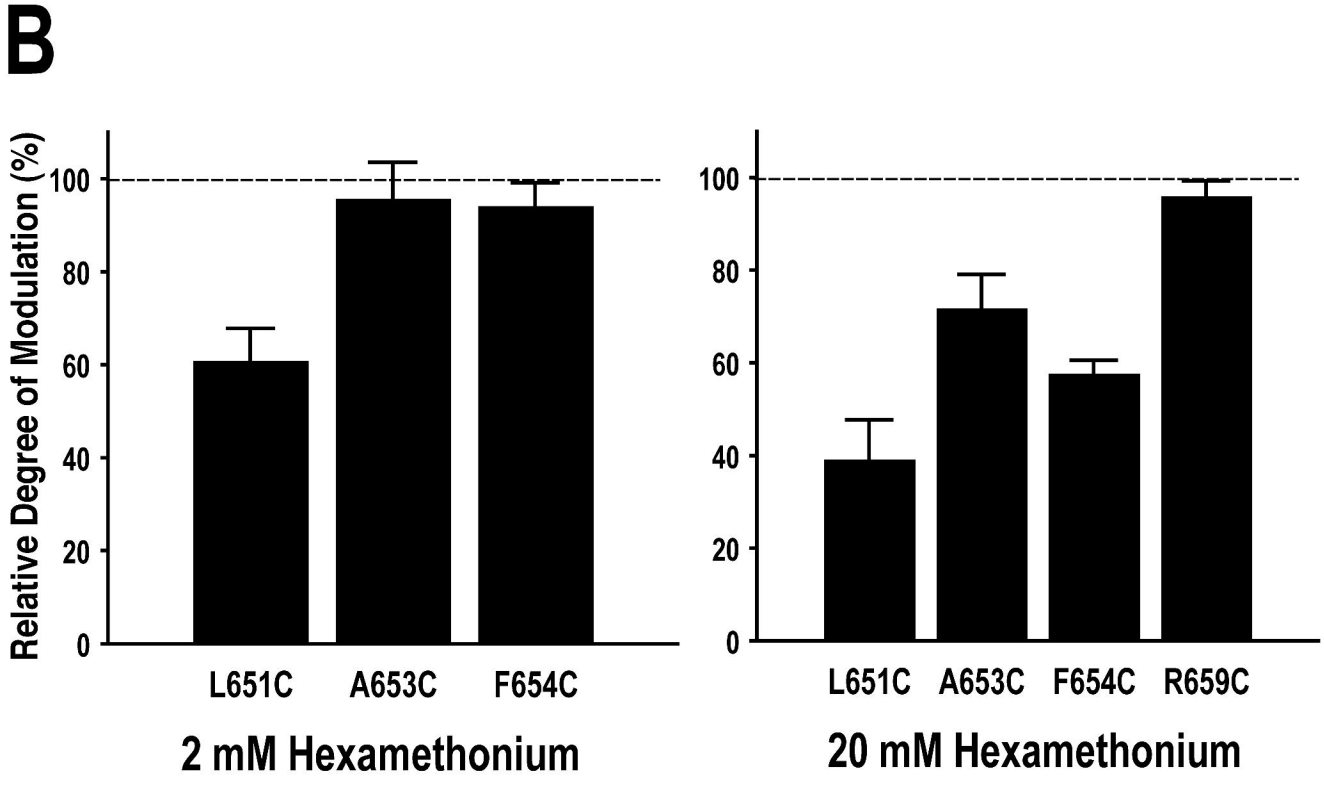
B
Relative Degree of Modulation (%)
100
80
60
40
20
0
L651C
A653C
F654C
2 mM Hexamethonium
100
80
60
40
20
0
L651C
A653C
F654C
R659C
20 mM Hexamethonium

Figure 6